Available online at www.sciencedirect.com
ScienceDirect
Catalysis Today 131 (2008) 477–482
CATALYSIS TODAY
www.elsevier.com/locate/cattod

# Re-investigating the CO oxidation mechanism over unsupported MnO, $Mn_2O_3$ and $MnO_2$ catalysts

Kanaparthi Ramesh, Luwei Chen, Fengxi Chen, Yan Liu, Zhan Wang, Yi-Fan Han *

*Institute of Chemical and Engineering Sciences (ICES), 1 Pesek Road, Jurong Island, Singapore 627833, Singapore*

Available online 26 November 2007

**Abstract**

Kinetic study of CO oxidation in combination with experiments of temperature-programmed oxidation (TPO) and reduction (TPR) have been performed on various unsupported crystalline manganese oxides ($MnO_x$); while the reactivity shows an order of $MnO \leq MnO_2 < Mn_2O_3$ in a mixture of unit ratio of $O_2$/CO at/below 523 K. We propose that under the current conditions the interaction of adsorbed CO and O is mainly responsible for $CO_2$ formation on $Mn_2O_3$ and $MnO_2$ catalysts, following either the Langmuir–Hinshelwood mechanism or Eley–Rideal mechanism. Meanwhile, direct evidence from transient CO oxidation suggests that the Mars-van-Krevelen mechanism may occur for all catalysts simultaneously, especially, it is predominant for the MnO catalyst. The evidence of structural modifications during reaction was confirmed by Raman spectra obtained from used MnO.


*Keywords:* CO oxidation; Manganese oxide; Kinetics; Mechanism; Raman spectra; TPR; TPO

## 1. Introduction

Catalytic oxidation of CO has long been studied on various manganese oxide ($MnO_x$) catalysts, e.g., unsupported $MnO_2$ [1,2], supported $MnO_x$ [3–7] and copper manganese oxide [8]. It still attracts considerable attentions from both academia and industry, due to the low cost of $MnO_x$ in contrast to the expensive noble metal catalysts. With the growing demands of the innovative technology, manganese oxides based catalysts may find a new application for the selective removal of CO in $H_2$-rich gas for fuel cells [9–11] and indoor air purification. An understanding of the reaction mechanism and its relationship with the surface structure is of great importance for the design of new generation combustion catalysts. Especially, $MnO_x$-based materials find the application as catalysts for the low temperature-combustion, for instance, below 523 K [12]. However, the relevant mechanism for CO oxidation on $MnO_x$ catalysts at low temperatures has rarely been addressed.

So far, several kinetic and mechanistic studies have contributed to CO oxidation on the $MnO_x$-based catalytic system. Among them, the Mars-van-Krevelen mechanism, thus, the adsorbed CO is reacted with the labile lattice oxygen [2–5,9] has been widely accepted for this reaction above ca. 773 K, as illustrated in Eq. (1). The reactivity is, likely, associated with the capacity of manganese to form various oxidation states, e.g., redox reaction of $Mn^{2+}/Mn^{3+}$ or $Mn^{3+}/Mn^{4+}$, and ''oxygen mobility'' in the oxide lattice. In contrast, Brooks [1] in a very early study proposed that oxidation of CO might proceed via a mechanism of Rideal type on a $MnO_2$ surface, thus, $CO_2$ was produced by the reaction between the radical CO and the lattice/gas phase oxygen.

$$CO(ads) + O^{2-}(lattice) + 2Mn^{4+/3+} \rightarrow CO_2(ads) + 2Mn^{3+/2+} \quad (1)$$

Nevertheless, the debate about the mechanism, e.g., does the redox reaction of Mn cations really occur in the reaction? And how does the oxidation state of Mn affect the catalytic activity or does the CO oxidation go through the Langmuir–Hinshelwood mechanism? And so forth, will be lasting due to the lack of effective technique for ''in situ'' observation of the reaction. To date, the studies in combination with kinetics and spectroscopy are still the most effective way to obtain the reaction information.

Contradictory results in the previous studies are possibly caused by the inconsistent composition of $MnO_x$ (mixture of

* Corresponding author.
*E-mail address:* han_yi_fan@ices.a-star.edu.sg (Y.-F. Han).

0920-5861/$ – see front matter © 2007 Elsevier B.V. All rights reserved.
doi:10.1016/j.cattod.2007.10.061

$Mn^{2+}$, $Mn^{3+}$ and $Mn^{4+}$, and interaction with other metal oxides, such $CeO_x$, $ZrO_2$) and diverse reaction conditions. Consequently, the obtained kinetics may not reflect the ''real'' behavior of $MnO_x$ catalysts under reaction conditions. Therefore, in the present study intrinsic reaction rates of CO oxidation are acquired on high purity of Mn(IV)$O_2$, $Mn_2$(III)$O_3$ and Mn(II)O oxides below 523 K and unit ratio of CO/$O_2$. Such reaction conditions may minimize the variation of the oxidation state of Mn at the surface. On the other hand, demonstration of the redox properties of surface Mn in the reaction has been carried out by using techniques of TPR, TPO, XPS and Raman spectroscopy. To the best of our knowledge, the reported results have been rarely addressed for this catalytic system.

## 2. Experimental

### 2.1. Catalyst property and reactivity measurements

High purity of $MnO_x$, MnO (Aldrich, 99.99%, 1.1 $m^2$/g), $Mn_2O_3$ (Aldrich, 99.999%, 4.0 $m^2$/g) and $MnO_2$ (Aldrich, 99.999%, 0.9 $m^2$/g) as received, were used as catalysts in the present study. Scanning electron microscopy (SEM, JEOL, JBM-6700F) revealed that all $MnO_x$ particles were randomly distributed in the range of 0.06–0.7 μm, corresponding to an average particles size of ∼0.5 μm.

The activity measurements were carried out in a micro-plug-flow reactor. Before each experiment, the catalyst was conditioned in situ by heating in an ultra-high purity of Helium (UHP) at 323 K (2 h, 30 ml/min). The reactions were carried out in space velocity in the range of 6000–18,000 $h^{-1}$ at one atmosphere pressure: 5.0 kPa CO, 5.0 kPa $O_2$ and He. The analysis of the reactants and products was done with an online GC (Shimadzu GC-14B) which is equipped with a carbosieves-II column. In the differential flow measurements, the conversion was maintained below ∼10% by diluting the catalyst with $SiO_2$. Each data point in kinetic study was collected after reaction 1 h. Absolute reaction rates were calculated for the average concentration of each component $\dot{c}_i$, at the in- and outlet of the reactor:

$$r_{CO} = \frac{6.02 \times 10^{23} \times \dot{c}_{CO,in} \times X_{CO} \times \dot{V}_{gas}}{m_{MnO_x}} \quad (2)$$

$$[\text{moles s}^{-1}\ \text{gMnO}_x{}^{-1}]$$

$m_{MnO_x}$ is the mass of $MnO_x$ in the reactor bed, $\dot{V}$ the total molar flow rate, $X_{co}$ the conversion of CO based on $CO_2$ formation, $\dot{c}_{CO}$ the concentration of CO in gas mixture, equal to $p_i/p_0$, $p_i$ the partial pressure of reactants and $p_0$ is the total pressure in the system.

### 2.2. Temperature programmed oxidation (TPO), temperature programmed reduction (TPR) and transient CO oxidation

Prior to the TPR/TPO experiments, $MnO_x$ (50 mg) was pretreated in UHP Ar at 323 K in a flow rate of 30 ml/min for 2 h to remove excess moisture. Experiments of TPR, TPO and transient CO oxidation were performed in a micro fixed-bed reactor, which is connected to GC-QMS (HPR-20, Hiden Analytical Ltd.); while masses (*m/e*: 2, 16, 18, 28, 32 and 44) were monitored, and the detection limits in Ar are 100 ppm for CO, 10 ppm for $CO_2$ and $H_2$, and less than 1 ppm for $O_2$. The temperature was increased in ramp rate of 10 K/min from 323 to 900 K with a linear heating in a carrier gas of $O_2$ (5.0 kPa + Ar) for TPO and $H_2$ (5.0 kPa + Ar) for TPR with total flow rate of 50 ml/min.

In a typical experiment of the transient CO oxidation, the catalyst (150 mg) was purged with $H_2$ ($H_2$ 5.0 kPa + Ar) at 473 K for 2 h before dosing CO (consecutive pulse of CO: each time 10 μml of CO 5.0 kPa + Ar). Additionally, the reduction of MnO with $H_2$ was also carried out at 900 K under the same conditions.

### 2.3. Laser Raman spectroscopy (LRS)

The dispersive Raman microscope employed in the present study was a JY Horiba LabRAM HR equipped with three laser sources (UV, Visible, and NIR), a confocal microscope, liquid nitrogen cooled charge-coupled device (CCD) and a multi-channel detector (256 × 1024 pixels). The visible 514.5 nm argon ion laser was selected to excite the Raman scattering. The laser power from the source is around 20 mW, but when it reached the samples, the laser output was reduced to around 6–7 mW after passing through filtering optics and microscope objective. A 100× objective lens was used and the acquisition time for each Raman spectrum was approximately 60–120 s depending on the sample. The Raman shift range acquired was in the range of 200–1200 $cm^{-1}$ with spectral resolution 1.7–2 $cm^{-1}$. Each spectroscopy was collected only after 100 scans.

### 2.4. X-ray photoelectron spectroscopy (XPS)

XPS measurements were performed on a VG ESCALAB 250 spectrometer, using Al Kα radiation (1486.6 eV, pass energy 20.0 eV). The base pressure of the instrument is $1 \times 10^{-9}$ Torr. The background contribution B (E) (obtained by shirley method) caused by inelastic process was subtracted, while the curve-fitting was performed with Gaussian–Lorentzian profile by an standard software. The binding energies (BEs) were calibrated using C1s peak at 285.0 eV. The instrument was also calibrated by using Au wire. XPS spectra were recorded at $\theta = 90^\circ$. The atomic ratios of oxygen/manganese (O/Mn) have been calculated from the equation [13,14]: $N_0/N_{Mn} = (I_0/S_0)/(I_{Mn}/S_{Mn})$, where the $I_{Mn}$ and $I_0$ are the time-normalized intensities of the Mn2p and O1s levels, and $S_0$ (0.711 for O1s) and $S_{Mn}$ (2.420 for Mn2p) are the atomic sensitivity factors for X-ray sources at 90°. The BEs O1s at 529.0–530.0 eV were selected as the contributions from manganese oxides [15].

## 3. Results and discussion

The $H_2$-TPR profiles of various bulk $MnO_x$ are shown in Fig. 1, which shows that the $H_2$-comsumption started around

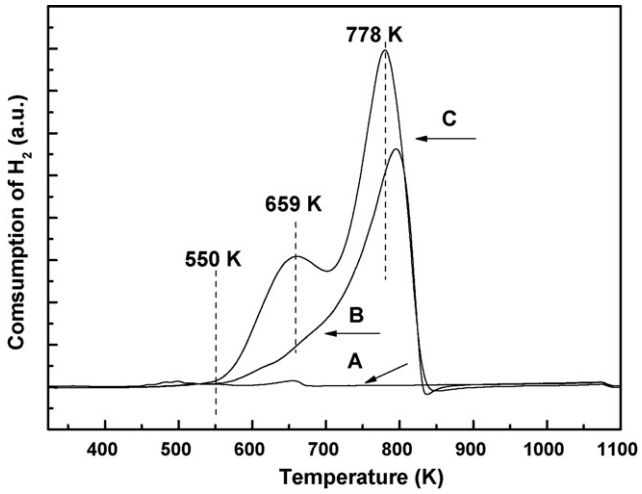


Fig. 1. TPR profiles of MnO (A), $Mn_2O_3$ (B) and $MnO_2$ (C) oxides in the mixture of $H_2$ (5.0 kPa)–Ar with a flow rate of 50 ml/min.

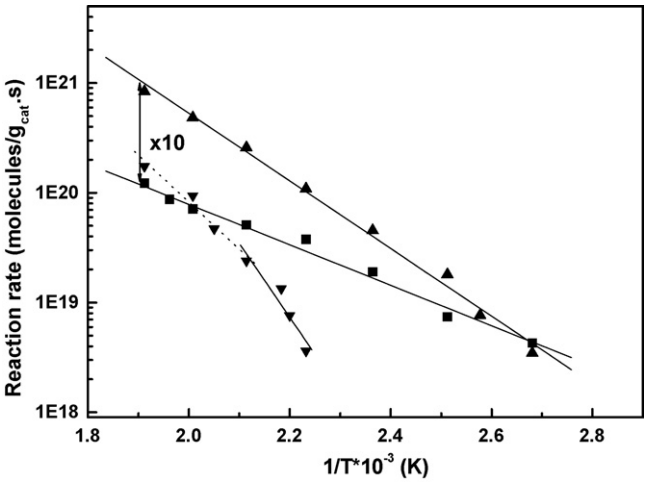


Fig. 3. Arrhenius plots from CO oxidation on the high purity of MnO (▼), $Mn_2O_3$ (■) and $MnO_2$ (▲) oxide catalysts, feed gas: CO (5.0 kPa) + $O_2$ (5.0 kPa), helium balance.

550 K for both $MnO_2$ and $Mn_2O_3$; however, detectable depletion of $H_2$ was not observed for MnO up to 900 K. The TPR of $MnO_2$ shows two overlapped peak maxima corresponding to the temperatures of 659 and 778 K. These two peaks can be attributed to the two-step reduction of $MnO_2$: the first step corresponds to the reduction of $MnO_2$ to $Mn_3O_4$ and the second step due to the further reduction of $Mn_3O_4$ to MnO. This result is in good agreement with the $H_2$-TPR results of $MnO_2$ reported in the literature [16]. Compared to that of $MnO_2$, the $Mn_2O_3$ showed single reduction peak corresponding temperature maxima at 778 K. However, it is very hard to define clear boundaries between the various regions. During the $H_2$-TPR, $Mn_2O_3$ reduces to $Mn_3O_4$ in the first step and further reduces to MnO. On the other hand, as illustrated in Fig. 2, $O_2$-TPO experiments reveal that oxidation of MnO starts at ca. 438 K followed a maximum at 881 K; while $Mn_2O_3$ is very stable in oxygen atmosphere till 1100 K. Therefore, under the reaction conditions at/below 523 K and unit ratio of $O_2$/CO the oxidation states of Mn on the surface should remain for

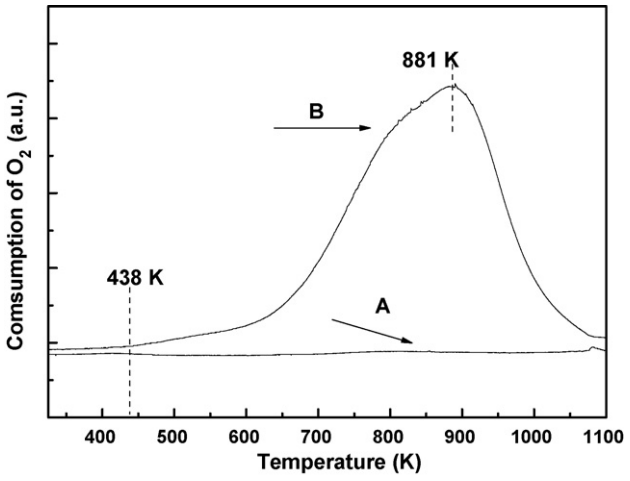


Fig. 2. TPO profiles of MnO (A) and $Mn_2O_3$ (B) in the mixture of $O_2$ (5.0 kPa)–Ar with a flow rate of 50 ml/min. The manganese oxides, as received, purged with Ar at 323 K for 2 h before heating, 10 K/min of the ramp rate.

$Mn_2O_3$ and $MnO_2$, and slight oxidation of Mn may occur for MnO as also evidenced with LRS spectra (see Fig. 4A).

Arrhenius plots in Fig. 3 show that the CO oxidation rate is strongly dependent on the reaction temperature in the region of 373–523 K. Onset of reaction can be observed at 373 K for both $Mn_2O_3$ and $MnO_2$, while the reactivity for $Mn_2O_3$ is higher than $MnO_2$ in the temperature range of 373–523 K. The rate-discrepancy for two catalysts increased with the rise of temperature, about an order of magnitude variation was measured at 523 K. In contrast, the reactivity for MnO catalyst was not observed until 448 K. Interestingly, this temperature also corresponds to where MnO start oxidizing during TPO. Among three catalysts, MnO exhibited the lowest reactivity in the temperature range of 448–473 K; but the rate for MnO became comparable to $MnO_2$ when the temperature was above 473 K. The apparent activation energies (Ea), for all catalysts and the values reported in the literature have been listed in Table 1. Arrhenius plots for MnO can be divided into two parts according to the relationship of log (rate) versus 1/*T*, corresponding to a Ea value of 129.1 kJ/mol in the range of 373–473 K and 81.6 kJ/mol in the range of 473–523 K. It is 1.5–3.0 times higher than that for $Mn_2O_3$ (57.9 kJ/mol) and $MnO_2$ (34.3 kJ/mol). The Ea for $MnO_2$ here is close to 26.7 kJ/mol obtained by Brooks [1]. In the similar conditions, Cracium [4] reported that Ea value was dependent on the size of $MnO_2$ particles, varying from 44.6 to 120 kJ/mol corresponding particle size in the range of 6.7–16.7 nm, which is higher than what we observed in the present study.

The LRS spectra, as shown in Fig. 4, together with the XRD patterns (not shown for the sake of brevity), revealed that the bulk structure of the $Mn_2O_3$ and $MnO_2$ catalysts corresponds to α- and β-type, respectively [17–19]. The LRS spectra from α-$Mn_2O_3$ shows bands at 312, 651 and 691 $cm^{-1}$ (Fig. 4B). The peaks from β-$MnO_2$ at 536, 668 and 762 $cm^{-1}$ are indicative of stretching mode of the $MnO_6$ octahedra (Fig. 4C). The bands at 309/310, 365, 502/472, and 641/651 $cm^{-1}$ detected for both fresh and spent catalysts may correspond to the out-of-plane bending modes of $MnO_x$, asymmetric stretch of bridge oxygen

Table 1
Apparent activation energy (Ea) for CO oxidation on unsupported $MnO_x$ catalysts and comparison with the literature data

| Catalysts | Ea (kJ/mol) | Temperature range (K) | Conditions | Ref. |
|---|---|---|---|---|
| MnO (bulk) | 129.1 ± 5.0 | 373–473 | $p_{CO}$: 2.5 kPa, $p_{O_2}/p_{CO} = 1.0$ | This study |
| | 81.6 ± 2.0 | 473–523 | | |
| $Mn_2O_3$ (bulk) | 57.9 ± 2.0 | 373–523 | $p_{CO}$: 2.5 kPa, $p_{O_2}/p_{CO} = 1.0$ | This study |
| $MnO_2$ (bulk) | 34.3 ± 2 | 373–523 | $p_{CO}$: 2.5 kPa, $p_{O_2}/p_{CO} = 1.0$ | This study |
| $MnO_2$ (bulk) | 26.7 | 448–573 | $p_{CO}$: 3.4–5.0 kPa, in air | [1] |
| $MnO_2/SiO_2$ ($d_{MNO_2}$ : 6.7−16.7 nm) | 44.6–120.0 | 433–573 | $p_{CO}$: 1.0 kPa, $p_{O_2}/p_{CO} = 1.1$ | [4] |
| $MnO_2/Al_2O_3$ | 104.0 | 448–515 | $p_{CO}$: 15.0 kPa, $p_{O_2}/p_{CO} = 1.0$ | [3] |

species (Mn–O–Mn), symmetric stretch of $MnO_x$ groups, respectively [19–22]. Fig. 4A shows that two new bands, 318 and 371 $cm^{-1}$, appeared for the spent MnO catalyst after 5 h reaction at 523 K, indicating that the phase was moderately modified during the reaction by forming $Mn_3O_4$-like species [20]. TPO spectra (Fig. 2) also indicated that the oxidation of MnO started at ca. 438 K in the oxygen atmosphere. Fig. 4B and C show the LRS spectra from the fresh and used $Mn_2O_3$ and $MnO_2$ catalysts. Obviously, the phases of $Mn_2O_3$ and $MnO_2$ were almost unchanged after reaction. Furthermore, from the LRS spectra we observed that pretreating the catalysts in the oxidative (5 kPa $O_2$ + Ar, 5 h, 523 K) or reductive (5 kPa CO + Ar, 5 h, 523 K) atmosphere has not changed the surface structure. It is interesting to note here that XRD of spent catalysts also proved that there was almost no variation for crystalline structures of $MnO_2$ and $Mn_2O_3$ catalysts.

Fig. 5 shows the Mn2p X-ray photoelectron spectra of various $MnO_x$. Table 2 presents the XPS results of binding energies (BE), full width at half maxima (FWHM) and surface atomic ratios of O/Mn of various $MnO_x$ catalysts before and after reaction. From Table 2 it can be concluded that there is no difference in terms of BE for both fresh and spent catalysts. The BE around 642.1 and 641.2 eV could be attributed to the presence of $Mn^{4+}$ and $Mn^{3+}$ species, respectively [23]. From Fig. 5 it can be seen that the bulk $MnO_2$ catalyst shows an asymmetric peak located at 642.1 eV (Mn2p3/2) indicating the presence of $Mn^{4+}$. The BEs of Mn3/2 shifted to lower values in the following order: $MnO_2 > Mn_2O_3 > MnO$. The variation of XPS binding energies of Mn2p alone, from $Mn^{2+}$ to $Mn^{4+}$, usually is too narrow (less than ca. 1.0 eV) to precisely evaluate the Mn valence in $MnO_x$, since the Mn2p features are relatively broad for all $MnO_x$ compounds. The assignment can be complicated further if the Mn in samples is present of several chemical states. So, the extent of Mn3s multiplet splitting measured simultaneously (Mn3sΔE) offers additional insights into the Mn chemical states. The oxidation states from Mn2p (column 2 in Table 2) and Mn3sΔE (column 4 in Table 2) for the fresh and spent catalysts are almost consistent.

As shown in Fig. 3, the reactivity of $MnO_x$ follows an order: $MnO \leq MnO_2 < Mn_2O_3$. Three factors, presumably, impact the reactivity of $MnO_x$ catalyst: (i) variation of Mn oxidation states, (ii) bonding labile lattice oxygen and (iii) retention of an oxidation products on the surface phase, such as $CO_2$ and $CO_3^{2-}$ [5]. For conciseness, here we confine our discussion mainly on the first factor. Adsorption of CO on $Mn^{2+}$, $Mn^{3+}$ and $Mn^{4+}$ at room temperature has been well proved by the infrared spectroscopy [5,24,25]. Cracium et al. [5] has found that $Mn^{2+}$–CO species are more stable than the $Mn^{3+}$–CO and $Mn^{4+}$–CO species due to a back π-donation only exist in the case of former. This seems to be the primary reason that MnO shows the lowest reactivity among three catalysts, because more energy is needed for activating the CO–$Mn^{2+}$ bond in the reaction. Consequently, MnO exhibited higher activation energy (Ea) than $Mn_2O_3$ and $MnO_2$ as listed in Table 1. A moderate fall of Ea for MnO at above 473 K may hint a subtle modification of mechanism at elevated temperatures. Moreover, higher Ea for MnO in contrast to $Mn_2O_3$ and $MnO_2$ indicated that oxidation of CO might go through quite different mechanism for those catalysts.

The LRS spectra show the structure of the surface phase was little affected in the reduction/oxidation (523 K). Based on the TPO and TPR results, we infer that the redox properties of Mn cations are unlikely to happen for the most of Mn on the $Mn_2O_3$ and $MnO_2$ surfaces under the current reaction conditions. The active oxygen for the oxidation of CO, at least for the type of catalysts, in this study, may not come from the lattice oxygen as

Table 2
Results of XPS for MnO, $Mn_2O_3$, $MnO_2$ catalysts

| Samples | BE Mn $2p_{3/2}$ (FWHM) (eV) | BE $Mn2p_{1/2}$ (FWHM) (eV) | Mn3sΔE (eV) | Mn oxidation states | O/Mn atomic ratios |
|---|---|---|---|---|---|
| MnO[a] | 641.2 (3.3) | 653.0 (3.3) | 6.3 | 2+ | 0.95 |
| MnO[b] | 641.2 (3.3) | 653.1 (3.2) | 6.4 | 2+ | 0.97 |
| $Mn_2O_3$[a] | 641.8 (3.0) | 654.1 (3.2) | 4.9 | 3+ | 1.67 |
| $Mn_2O_3$[b] | 641.8 (3.0) | 654.2 (3.1) | 5.0 | 3+ | 1.65 |
| $MnO_2$[a] | 642.1 (2.2) | 654.5 (2.7) | 4.5 | 4+ | 1.93 |
| $MnO_2$[b] | 642.3 (2.3) | 654.5 (2.6) | 4.5 | 4+ | 2.0 |

[a] Prior to XPS measurement catalysts (fresh) were dehydrated at 393 K for 2 h in a He flow rate of 20 ml/min.
[b] Spent catalysts were from CO oxidation at 473 K for 10 h in a mixture of CO (5.0 kPa), $O_2$ (5.0 kPa) and Ar under a space velocity: 18,000 $h^{-1}$.

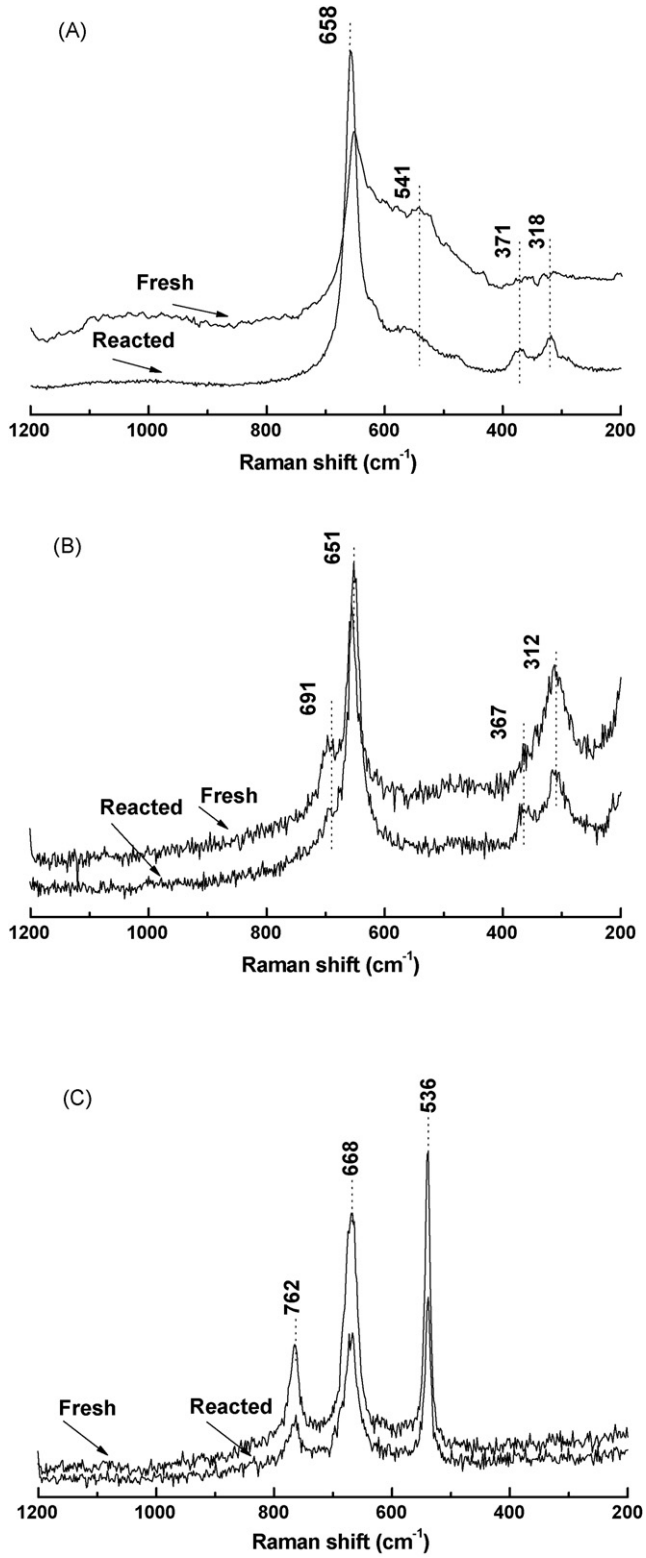


Fig. 4. Laser Raman spectra of (A) MnO, (B) $Mn_2O_3$ and (C) $MnO_2$ under ambient conditions, fresh: purged in 30 ml/min He at 323 K for 2 h; reacted: reacted in mixture of CO (5.0 kPa) + $O_2$ (5.0 kPa), helium balance, at 523 K with a flow rate of 30 ml/min for 5 h.

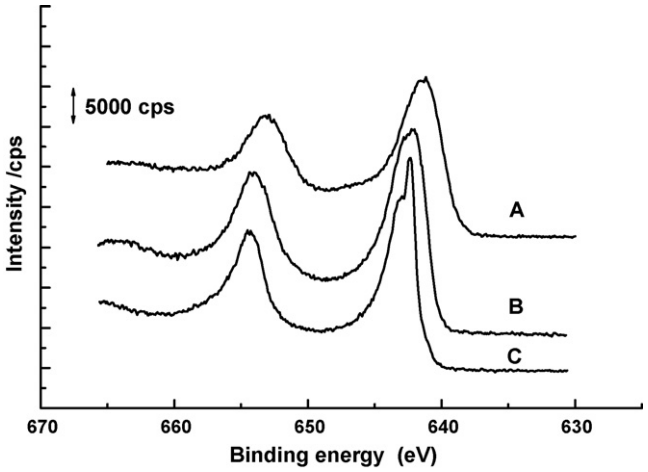


Fig. 5. X-ray photoelectron spectra of MnO (A), $Mn_2O_3$ (B) and $MnO_2$ (C) catalysts.

popularly accepted view of point, instead, from adsorbed oxygen. That is to say, the Langmuir–Hinshelwood mechanism is supposed to be responsible for this reaction.

For the purpose above-mentioned, subsequently, we performed the transient CO oxidation for all catalysts with a "net" surface, which is lean for the adsorbed oxygen. The removal of adsorbed oxygen from the surface of catalysts was done by reacting with $H_2$ at 473 K (purging with $H_2$ for 2 h); then dosing CO only less than 10% conversion of CO was observed for $MnO_2$ and $Mn_2O_3$, but complete conversion of CO observed for MnO. Especially, the formation of $CO_2$ was detected for MnO at the same temperature after treating at 900 K in $H_2$ for 2 h. Therefore, CO oxidation may mainly go through the Mars-van-Krevelen mechanism on the MnO catalyst. However, the same mechanism may not be ruled out for $Mn_2O_3$ and $MnO_2$ due to the occurrence of redox reaction for the small fraction of Mn cations at the top layers of the surface.

The adsorption of oxygen on the surface defects has been widely demonstrated for the transition metal oxides [26,27]. We assume that the number of the surface defects for $MnO_2$ and $Mn_2O_3$ may be higher than that for MnO. Thus, the extremely low Ea value is understandable for the $MnO_2$ and $Mn_2O_3$ in comparison with that for MnO catalysts, because more energy during the reaction is required for the mobility of lattice oxygen for MnO. In particular, the creation of $Mn_3O_4$-like species for the reacted MnO, as observed from the LRS spectra (Fig. 4A), might be an indirect evidence for the redox of $Mn^{2+}/Mn^{3+}$ on MnO surface phase during the reaction.

For the same reaction on $MnO_x$/support catalysts, Cracium et al. [5] suggested that $Mn^{3+}$ and $Mn^{2+}$ were weaker catalytic active sites than $Mn^{4+}$ sites, it led to the relatively higher reactivity for $MnO_2$ than $Mn_2O_3$ and MnO above 573 K. It is contradictory to our observations: the reactivity of $Mn_2O_3$ is superior to MnO and $MnO_2$ as illustrated in Fig. 3. The high reactivity for $Mn_2O_3$ may be attributed to not only the moderate strength of CO–$Mn^{3+}$ bond but also the abundant defects/oxygen vacancies on its surface phase [27]. Similarly, in the study of NO decomposition over the catalysts of $Mn_2O_3$ and $Mn_3O_4$ Vannice and Yamashita [28–30] also suggested that the

route for reaction might proceed via the Langmuir–Hinshelwood mechanism, but the temperature need to be greater than 773 K. Moreover, they observed that the $Mn_2O_3$ released more lattice oxygen than other $MnO_x$ in a TPD experiment.

In summary, the preliminary results in this study suggests that under the restrict conditions (at/below 523 K and unit ratio of $O_2$/CO) CO oxidation may proceed via the interaction between adsorbed CO and O (Langmuir–Hinshelwood mechanism) on the bulk $Mn_2O_3$ and $MnO_2$ catalysts; while the reaction of adsorbed CO with the lattice oxygen (Mars-van-Krevelen mechanism) is primarily responsible for $CO_2$ formation on the MnO catalyst. In addition, the catalytic reactivity for those Mn oxides can be affected by the oxidation states of Mn cations in the low temperature CO oxidation.

## 4. Conclusions

Different structures of $MnO_x$ were tested for the low temperature CO oxidation reaction. The catalytic reactivity followed the trend of $MnO \leq MnO_2 < Mn_2O_3$ in a mixture of unit ratio of $O_2$/CO at/below 523 K. $H_2$ TPR results showed that $MnO_2$ reduces to MnO in two subsequent steps via forming $Mn_3O_4$. TPR, TPO and XPS studies showed that under the reaction conditions at/below 523 K and unit ratio of $O_2$/CO the oxidation states of Mn on the surface remain for $Mn_2O_3$ and $MnO_2$. However, a slight oxidation of MnO during the reaction was observed by TPO and this result was further confirmed by the LRS spectra. Under the restrict conditions CO oxidation may follow the Langmuir–Hinshelwood mechanism on the bulk $Mn_2O_3$ and $MnO_2$ catalysts; while for the MnO catalyst the reaction primarily follow the Mars-van-Krevelen mechanism.

## References

[1] C.S. Brooks, J. Catal. 8 (1967) 272.
[2] M.I. Zaki, M.A. Hasan, L. Pasupulety, K. Kumari, Thermochim. Acta 311 (1998) 97.
[3] J. Mooi, P.W. Selwood, J. Am. Chem. Soc. 74 (1952) 2461.
[4] R. Cracium, Catal. Lett. 55 (1998) 25.
[5] R. Cracium, B. Nentwick, K. Hadjiivanov, H. Knözinger, Appl. Catal. A: Gen. 243 (2003) 67.
[6] Y.-F. Han, F. Chen, Z.-Y. Zhong, K. Ramesh, E. Widjaja, L.-W. Chen, Catal. Commun. 7 (2006) 739.
[7] Y.-F. Han, F. Chen, Z.-Y. Zhong, K. Ramesh, L.-W. Chen, E. Widjaja, J. Phys. Chem. B 110 (2006) 24450.
[8] G.J. Hutchings, A.A. Mirzaei, R.W. Joyner, M.R.H. Siddiqui, S.H. Taylor, Appl. Catal. A: Gen. 166 (1998) 143.
[9] H. Knözinger, Heterogeneous catalysis and solid catalysts, in: Ullmann's Encyclopedia of Industrial Chemistry, Wiley-VCH Verlag GmbH & Co. KGaA., 2002.
[10] Y. Teng, H. Sakurai, A. Ueda, T. Kobayashi, Int. J. Hydrogen Energy 24 (1999) 355.
[11] Y.-F. Han, M. Kahlich, M. Kinne, R.J. Behm, Appl. Catal. B 50 (2004) 209.
[12] Y.-F. Han, Z.-Y. Zhong, L.-W. Chen, E. Widjaja, F. Chen, Y. Liu, Z. Wang, Singapore International Chemical Conference 4, 8–10 December 2005, Singapore, (2005), p. 72.
[13] J.H. Scofield, J. Electron. Spectrosc. Relat. Phenom. 8 (1976) 129.
[14] J.F. Moulder, W.F. Stickle, P.E. Sobol, K.D. Bomben, in: J. Chastain, C. King, Jr. (Eds.), Handbook of X-ray Photoelectron Spectroscopy, Physical Electronics, Inc., 1995, ISBN: 0-9648124-1-X.
[15] S.-J. Lee, A. Gavriilidis, Q.A. Pankhurst, A. Kyek, F.E. Wagner, P.C.L. Wong, K.L. Yeung, J. Catal. 200 (2001) 298.
[16] J. Carno, M. Ferrandon, E. Bjonbom, S. Jaras, Appl. Catal. 155 (1997) 265.
[17] C. Julien, M. Massot, S. Rangan, M. Lemal, D. Guyomard, J. Raman Spectrosc. 33 (4) (2002) 223.
[18] F. Kapteijn, A.D. van Langeveld, J.A. Moulijn, A. Andreini, M.A. Vuurman, A.M. Turek, J.M. Jehng, I.E. Wachs, J. Catal. 150 (1994) 94.
[19] M.C. Bernard, A. Hugot-Le Goff, B.V. Thi, S. Cordoba de Torresi, J. Electrochem. Soc. 140 (1993) 3065.
[20] F. Buciuman, F. Patcas, R. Cracium, D.R.T. Zahn, Phys. Chem. Chem. Phys. 1 (1999) 1.
[21] Y.T. Chua, P.C. Stair, I.E. Wachs, J. Phys. Chem. B 105 (2001) 8600.
[22] J.M. Chalmers, P.R. Riffiths (Eds.), Handbook of Viberational Spectroscopy, Jim Wilkie, J & R Press, UK, 2002.
[23] J. Rosso, M.F. Hochella Jr., Surf. Sci. Spectra 4 (1998) 253; M.A. Stranick, Surf. Sci. Spectra 6 (1999) 39.
[24] G.P. Harrison, E.W. Thornton, J. Chem. Soc. Faraday Trans. 75 (1979) 1487.
[25] M. Kantcheva, M.U. Kucukkal, S. Suzer, J. Catal. 190 (2000) 144.
[26] Z. Yan, S. Chinta, A.A. Mohamed, J.P. Fackler Jr, D.W. Goodman, J. Am. Chem. Soc. 127 (2005) 1604.
[27] M. Fernandez-Garcia, A. Martinez-Arias, J.C. Hanson, J.A. Rodriguez, Chem. Rev. 104 (2004) 4063.
[28] T. Yamashita, M.A. Vannice, J. Catal. 161 (1996) 254.
[29] T. Yamashita, M.A. Vannice, J. Catal. 161 (1996) 158.
[30] T. Yamashita, M.A. Vannice, Appl. Catal. B: Environ. 13 (1997) 141.